Air Bearing Table Mechanization and Verification of a Spacecraft Wide-Angle Attitude Control System

FRANCIS J. MORAN* AND BRUCE H. DISHMAN*
NASA Ames Research Center, Moffett Field, Calif.

The problem of controlling the attitude of a space vehicle slewing through large angles in three dimensions is experimentally investigated. The investigation is based on a control system synthesized from Euler's theorem on rotation which states that any attitude change of a rigid body may be accomplished by a single rotation about a properly chosen axis. A theoretical analysis showed that a system using the control law has global stability. The investigation was carried out using an air bearing table to simulate the spacecraft, two gimbaled star trackers as position sensors, rate gyroscopes to provide damping information, and reaction wheels as control torquers. An on line digital computer acts as a real time controller which determines the control axis orientation from star tracker gimbal outputs, and generates simultaneous commands to the three torquers. The experimental results show that the control system was stable while slewing through large angles and had excellent pointing accuracy.

Nomenclature

$\bar{a}_1,\bar{a}_2,\bar{a}_3$ = triad of unit orthogonal vectors attached to the vehicle marked axes defining the vehicle coordinate system; which form a right-handed coordinate system

A_i,A_0 = inner and outer gimbal angles of star tracker number three; they define the orientation of $\bar{T}_3$ at time $t > 0$; $A_i(0)$, and $A_0(0)$ are initial values

A_{as} = 3×3 direction cosine matrix defining the orientation of the vehicle coordinate system with respect to the reference inertial coordinate system

$\dot{A}_{as}$ = time derivative of matrix A_{as}; $A_{as}(0)$ = initial value

A_{ds} = 3×3 direction cosine matrix defining the orientation of the commanded vehicle position with respect to the reference inertial coordinate system

B_a,B_s = 3×3 nonorthogonal matrices defining the orientation of the composite tracker coordinate system with respect to the vehicle coordinate system and the reference inertial coordinate system, respectively

c_0,c = unit eigenvectors of the vehicle attitude error matrix at $t = 0$ and $t > 0$, respectively

$c(1),c(2),c(3)$ = components of the eigenvector $\bar{c}$ in the body roll, pitch, and yaw axes, respectively

$\bar{d}_1,\bar{d}_2,\bar{d}_3$ = triad of unit orthogonal vectors defining the commanded position of the vehicle coordinate system; this forms a right-handed coordinate system

$J_a(1),J_a(2),J_a(3)$ = vehicle moment of inertia measured about the $\bar{a}_1$, $\bar{a}_2$, $\bar{a}_3$ axes, respectively

$J_a(\max)$ = maximum value of J_a (J_3 for this paper)

K_i,K_0 = inner and outer gimbal angles of star tracker number two. They define the orientation of $\bar{T}_2$ at time $t > 0$; $K_i(0)$, and $K_0(0)$ are initial values

$K_1(1),K_1(2),K_1(3)$ = gain terms associated with the control law about the body roll, pitch, and yaw axes, respectively, $K_1(\mathrm{I}) = [J_a(I)Z_a(\max)/J_a(\max)]I = 1,2,3$

K_2 = rate gain term associated with the control law, $1/\omega_a(\max)$

$q(1),q(2),q(3)$ = $c(I) \sin \Phi$ I = 1,2,3

R = 3×3 direction cosine matrix defining the orientation of the vehicle coordinate system with respect to the commanded coordinate system (error matrix)

$\bar{s}_1,\bar{s}_2,\bar{s}_3$ = triad of unit orthogonal vectors defining the reference coordinate system. Considered to be inertially fixed. This forms a right-handed coordinate system

$S(x)$ = skew symmetric matrix defined for any 3×1 column matrix

$$\text{if } x = \begin{matrix} X_1 \\ X_2 \\ X_3 \end{matrix}$$

$$\text{then } S(x) = \begin{matrix} 0 & X_3 & -X_2 \\ -X_3 & 0 & X_1 \\ X_2 & -X_1 & 0 \end{matrix}$$

$\bar{T}_{21},\bar{T}_{22},\bar{T}_{23}$ = triad of unit orthogonal vectors defining this orientation of star tracker number two. This forms a right-handed coordinate system

$\bar{T}_{31},\bar{T}_{32},\bar{T}_{33}$ = triad of unit orthogonal vectors defining the orientation of star tracker number three; this forms a right-handed coordinate system

$\bar{T}_1,\bar{T}_2,\bar{T}_3$ = composite tracker coordinate system; nonorthogonal triad of unit vectors defining the lines of sight of the star trackers; forming a right-handed coordinate system

$Z_a(1),Z_a(2),Z_a(3)$ = control voltages about the vehicles roll, pitch, and yaw axes, respectively

$Z_a(\max)$ = maximum value of control voltage

Φ,Φ_s = Euler rotation angle of the error matrix R, and value of Φ at which Z_a saturates

Φ_{LARGE} = $5° \leq \Phi \leq 180°$

Φ_{SMALL} = $0 \leq \Phi < 5°$ arbitrary gain term selected to show the control system nulling characteristics

$Sat(\Phi,\Phi_s)$ = 1 if $\Phi \geq \Phi_s$, or Φ/Φ_s if $\Phi < \Phi_s$

ψ,ϕ,θ = air bearing table yaw, roll, and pitch Euler angles

ψ_k,ϕ_k,θ_k = known air bearing table yaw, roll, and pitch Euler angles

$\omega_a(1),\omega_a(2),\omega_a(3)$ = body inertial angular rates about the $\bar{a}_1$, $\bar{a}_2$, and $\bar{a}_3$ axes, respectively

$\omega_a(\max)$ = maximum body inertial rate

Presented as Paper 69-856 at the AIAA Guidance, Control, and Flight Mechanics Conference, Princeton, N.J., August 18–20, 1969; submitted August 28, 1969; revision received February 16, 1970.

* Research Scientist.

— = overline indicating a vector quantity
0 = initial value
$c\theta$, $s\theta$ = $\cos\theta$ and $\sin\theta$, respectively

Introduction

THE need for a system which insures stability while controlling the rotational position of a rigid body slewing through large angles presents itself in a program such as the Orbiting Astronomical Observatory (OAO). The problem here is to point a telescope, rigidly attached to the vehicle, in any direction dictated by a ground-based observer. The present OAO program accomplishes wide angle slewing by commanding the vehicle in an Euler sequence. The slew control system is open loop and drives the vehicle to within the limits of the coarse control system. Then the coarse control system stabilizes the vehicle by resolving the star tracker gimbal angles into the proper components to drive the vehicle to within the field of view of the fine sensor.

This analysis is concerned with the experimental investigation of an attitude control system which allows simultaneous rotation about all three body axes, has proven global stability, and drives the vehicle to within the range of the fine sensor. The control law is synthesized from Euler's theorem on rotation which states that any attitude change of a rigid body may be accomplished by a single rotation about a properly chosen axis. This axis of rotation is the eigenvector of the direction cosine matrix defining the orientation of the body's present position with respect to the commanded position.

The control system simulation was performed on a three degrees-of-freedom air bearing table. Two gimballed star trackers, mounted with their outer gimbal axes parallel to the table roll axis, were used as attitude sensors. These trackers have angular freedom of $\pm 50°$ about their inner and outer gimbal axes. Reaction wheels, driven by d.c. motors, were used as control torquers. A digital computer was used as an on-line controller for the table. This computer performed the necessary matrix operations on the star tracker position information and generated the three control signals to drive the torquers.

Experimental Apparatus

The mechanization of this technique of attitude control was carried out on a three degrees-of-freedom air bearing table. This facility is shown in Fig. 1. The air bearing table is housed in a spherical chamber which can be evacuated to a pressure of 1 mm of mercury. The chamber and air bearing table assembly are supported on a seismic foundation.

The air bearing table rests on a 7-in.-diam stainless steel ball which is supported by a cushion of air injected into a mating socket. The table and control system configuration used in this analysis had a weight of 1800 lb, and an inertia of

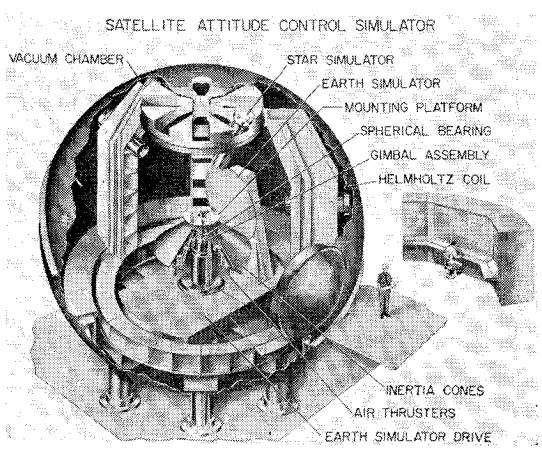

Fig. 1 Satellite attitude control simulator.

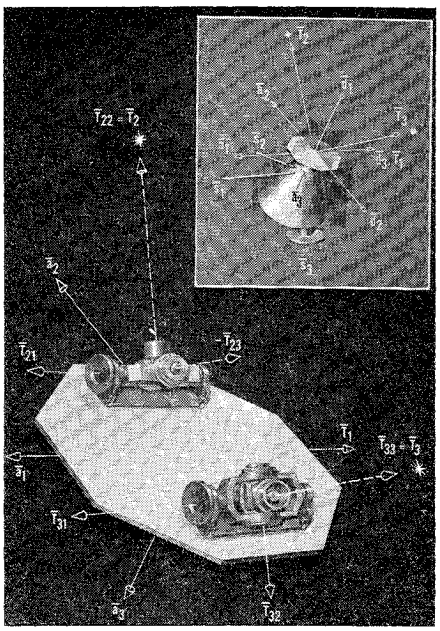

Fig. 2 Orientation of coordinate systems.

145 slug-feet^2 about the pitch and roll axes and 180 slug-feet^2 about the yaw axis. The air bearing table has unlimited freedom of motion about the yaw axis and is limited to $\pm 29°$ about the pitch and roll axes.

Communications with the table and power to the table are transmitted via a mercury pool and slipring assembly. From the table, signals pass through individual pins arranged in a circle and located on the table. The pins project into individual pools of mercury located on a following gimbal system. (The following gimbal system tracks the table by utilizing a three axis autocollimating error detection system.) From the base of the mercury pools, the signals then pass through a slipring assembly located on the yaw gimbal. The sliprings allow unlimited motion in yaw. This technique of getting data on and off the table eliminates the disturbance torques which would be caused by hanging wires from above the table and/or the complexity of telemetering the data.

Table position information used in generating the control signals is derived from two gimballed star trackers. These trackers are located on the table in a manner such that their outer gimbal axes are parallel and aligned with the table roll axis. The trackers have angular freedom of $\pm 50°$ about both the inner and outer gimbal axes and use resolvers as gimbal angle readout devices. These resolvers have an accuracy of 5 min of arc. The star trackers have a max slewing rate of 0.75°/sec.

The trackers are locked onto simulated stars located within the air bearing chamber. These star simulators have a clear aperture of 12 in. and provide a star beam collimated to within ± 5 arc sec relative to the optical axis. The apparent star magnitude can be adjusted from -2.0 to 6.5.

Control torques were generated by three reaction wheels located along the three axes of the table. These reaction wheels were driven by 25-in. oz d.c. torque motors. The motor reaction wheel combination has a time constant of 35 sec and a max speed of 310 rad/sec.

The outputs from the two star trackers, the three rate gyros, and the three reaction wheel tachometers were sent in analog form to a digital computer. This computer acts as a real time controller for the air bearing table in that it accepts the basis analog signals, converts them to digital data, and performs the necessary matrix operations to generate the specified control law. Operational changes in the control law were easily carried out in the computer since it was programed in Fortran. The system program was cycled through the computer at a frequency of 30 Hz. The control signals gen-

erated by the computer were transmitted in analog form to the power amplifiers which drive the reaction wheels.

Vehicle Attitude Control

The attitude control problem consists of specifying a control law which will force the present attitude of the vehicle, given by a 3 × 3 direction cos matrix defined as A_{as}, to the commanded attitude, given by a 3 × 3 direction cos matrix defined as A_{ds}. The orientation of the present vehicle attitude and the commanded vehicle attitude is shown in Fig. 2. The coordinate system of the commanded position to which the vehicle is to slew is $(\bar{d}_1,\bar{d}_2,\bar{d}_3)$. The coordinate system oriented along the marked axes of the vehicle is $(\bar{a}_1,\bar{a}_2,\bar{a}_3)$. The inertial coordinate system to which all vehicle motion is referenced is $(\bar{s}_1,\bar{s}_2,\bar{s}_3)$.

The vehicle orientation and command orientation are expressed in terms of the inertial coordinate system by

$$\begin{pmatrix}\bar{a}_1\\ \bar{a}_2\\ \bar{a}_3\end{pmatrix} = (A_{as})\begin{pmatrix}\bar{s}_1\\ \bar{s}_2\\ \bar{s}_3\end{pmatrix}\begin{pmatrix}\bar{d}_1\\ \bar{d}_2\\ \bar{d}_3\end{pmatrix} = (A_{ds})\begin{pmatrix}\bar{s}_1\\ \bar{s}_2\\ \bar{s}_3\end{pmatrix} \tag{1}$$

From these relationships and the fact that A_{ds} is an orthogonal matrix ($A_{ds}^{-1} = A_{ds}^{t}$) it follows that the position of the vehicle with respect to the commanded position is given by

$$\begin{pmatrix}\bar{a}_1\\ \bar{a}_2\\ \bar{a}_3\end{pmatrix} = (A_{as})(A_{ds})^{t}\begin{pmatrix}\bar{d}_1\\ \bar{d}_2\\ \bar{d}_3\end{pmatrix} \tag{2}$$

This shows that the vehicle attains the commanded attitude when the matrix product $(A_{as})(A_{ds})^t$ forms an identity matrix. The matrix product $(A_{as})(A_{ds})^t = R$ is defined as the error matrix. The control law information will be extracted from this matrix.

Vehicle Attitude Determination

Since A_{ds} is specified, the problem is to determine the elements of A_{as}. This information is obtained by use of two star trackers on board the vehicle which are locked onto known stars; that is, stars whose position in the inertial reference frame is known. The line of sight to the first star will be denoted by a unit vector $\bar{T}_2$. The line of sight to the second star will be denoted by a unit vector $\bar{T}_3$. In order to utilize 3 × 3 matrix transformations in the mathematical analysis of vehicle attitude, it is necessary to generate a fictitious third line of sight from the vector cross product of $\bar{T}_2$ and $\bar{T}_3$: $\bar{T}_1 = \bar{T}_2 \times \bar{T}_3$.

The set of unit vectors $(\bar{T}_1,\bar{T}_2,\bar{T}_3)$ represent a nonorthogonal coordinate frame. The relation of this frame to the $\bar{s}$ and $\bar{a}$ coordinate systems can be given by the following two equations

$$\begin{pmatrix}\bar{T}_1\\ \bar{T}_2\\ \bar{T}_3\end{pmatrix} = (B_s)\begin{pmatrix}\bar{s}_1\\ \bar{s}_2\\ \bar{s}_3\end{pmatrix}\begin{pmatrix}\bar{T}_1\\ \bar{T}_2\\ \bar{T}_3\end{pmatrix} = (B_a)\begin{pmatrix}\bar{a}_1\\ \bar{a}_2\\ \bar{a}_3\end{pmatrix} \tag{3}$$

The matrices B_s and B_a are 3 × 3 arrays whose rows are the components of the $\bar{T}$ vectors as seen in the $\bar{s}$ and $\bar{a}$ coordinate systems, respectively. If it is assumed that the star trackers track perfectly and the stars are located at an infinite distance then the tracker coordinate system $(\bar{T}_1,\bar{T}_2,\bar{T}_3)$ is inertially fixed and the B_s matrix is a constant. The B_a matrix varies with vehicle orientation. Combining Eqs. (4) and (5) yields

$$\begin{pmatrix}\bar{s}_1\\ \bar{s}_2\\ \bar{s}_3\end{pmatrix} = (B_s^{-1})(B_a)\begin{pmatrix}\bar{a}_1\\ \bar{a}_2\\ \bar{a}_3\end{pmatrix} \tag{4}$$

From Eqs. (4) and (1) and the fact that A_{as} is an orthogonal matrix:

$$A_{as}^{t} = B_s^{-1}B_a \tag{5}$$

The problem is now to determine the elements of the B_s and B_a matrices in terms of the measured star tracker gimbal angles. This is done by a series of matrix transformations which orient the two gimballed star trackers with respect to the body and inertial coordinate systems.

The two star trackers were oriented on the air bearing table such that their outer gimbal axes were parallel to the vehicle roll axis, $\bar{a}_1$. The line of sight vector $\bar{T}_2$ is one of a set of three unit vectors $(\bar{T}_{21},\bar{T}_{22},\bar{T}_{23})$ which represents an orthogonal coordinate frame attached to a tracker designated as tracker number 2 ($\bar{T}_2 = \bar{T}_{22}$). Similarly, $\bar{T}_3$ is one of a set of three unit vectors $(\bar{T}_{31},\bar{T}_{32},\bar{T}_{33})$ which represent an orthogonal coordinate frame attached to a tracker designated as tracker number 3 ($\bar{T}_3 = \bar{T}_{33}$). Figure 2 shows the star trackers and their orientation on the air bearing table top. Tracker number 2 has its line of sight along the positive pitch axis of the body, $(\bar{a}_2)$, when its gimbal angles are zero. Tracker number three's line of sight points along the bodies negative yaw axis, $-\bar{a}_3$, when its gimbal angles are zero. The orientations of trackers two and three with respect to the vehicle coordinate frame are given by:

$$\begin{pmatrix}\bar{T}_{21}\\ \bar{T}_{22}\\ \bar{T}_{23}\end{pmatrix} = X(K_i)V(K_0)Y(1)\begin{pmatrix}\bar{a}_1\\ \bar{a}_2\\ \bar{a}_3\end{pmatrix} \tag{6}$$

$$\begin{pmatrix}\bar{T}_{31}\\ \bar{T}_{32}\\ \bar{T}_{33}\end{pmatrix} = W(A_i)V(A_0)Y(2)\begin{pmatrix}\bar{a}_1\\ \bar{a}_2\\ \bar{a}_3\end{pmatrix} \tag{7}$$

Table 1 Transformation matrices

$$V(K_0) = \begin{pmatrix}1 & 0 & 0\\ 0 & CK_0 & SK_0\\ 0 & -SK_0 & CK_0\end{pmatrix} \qquad V[K_0(0)] = \begin{pmatrix}1 & 0 & 0\\ 0 & CK_0(0) & SK_0(0)\\ 0 & -SK_0(0) & C[K_0(0)]\end{pmatrix}$$

$$V(A_0) = \begin{pmatrix}1 & 0 & 0\\ 0 & CA_0 & SA_0\\ 0 & -SA_0 & CA_0\end{pmatrix} \qquad V[A_0(0)] = \begin{pmatrix}1 & 0 & 0\\ 0 & CA_0(0) & SA_0(0)\\ 0 & -SA_0(0) & CA_0(0)\end{pmatrix}$$

$$X(K_i) = \begin{pmatrix}CK_i & SK_i & 0\\ -SK_i & CK_i & 0\\ 0 & 0 & 1\end{pmatrix} \qquad C[K_i(0)] = \begin{pmatrix}CK_i(0) & SK_i(0) & 0\\ -SK_i(0) & CK_i(0) & 0\\ 0 & 0 & 1\end{pmatrix}$$

$$W(A_i) = \begin{pmatrix}CA_i & 0 & -SA_i\\ 0 & 1 & 0\\ SA_i & 0 & CA_i\end{pmatrix} \qquad W[A_i(0)] = \begin{pmatrix}CA_i(0) & 0 & -SA_i(0)\\ 0 & 1 & 0\\ SA_i(0) & 0 & CA_i(0)\end{pmatrix}$$

$$Y(1) = \begin{pmatrix}1 & 0 & 0\\ 0 & 1 & 0\\ 0 & 0 & 1\end{pmatrix} \qquad Y(2) = \begin{pmatrix}1 & 0 & 0\\ 0 & -1 & 0\\ 0 & 0 & -1\end{pmatrix}$$

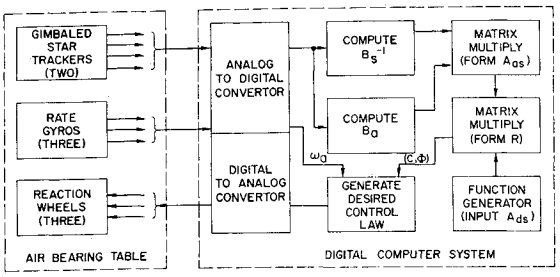

Fig. 3 Block diagram of the control system.

The transformation matrices $X(K_i)$, $V(K_0)$, $Y(1)$, $W(A_i)$. $V(A_0)$, and $Y(2)$ are defined in Table 1. From the above two equations, $\bar{T}_{22}$ and $\bar{T}_{33}$ are the second and third rows of the B_a matrix. The first row is $\bar{T}_1 = \bar{T}_2 \times \bar{T}_3$.

The orientations of trackers two and three with respect to the inertial reference frame are given by

$$\begin{pmatrix} \bar{T}_{21} \\ \bar{T}_{22} \\ \bar{T}_{23} \end{pmatrix} = X[K_i(0)]V[K_0(0)]Y(1)A_{as}(k)\begin{pmatrix} \bar{S}_2 \\ \bar{S}_2 \\ \bar{S}_3 \end{pmatrix} \quad (8)$$

$$\begin{pmatrix} \bar{T}_{31} \\ \bar{T}_{32} \\ \bar{T}_{33} \end{pmatrix} = W[A_i(0)]V[A_0(0)]Y(2)A_{as}(k)\begin{pmatrix} \bar{S}_1 \\ \bar{S}_2 \\ \bar{S}_3 \end{pmatrix} \quad (9)$$

where

$$A_{as}(K) = \begin{pmatrix} C\theta_k & 0 & -S\theta_k \\ 0 & 1 & 0 \\ S\theta_k & 0 & C\theta_k \end{pmatrix}\begin{pmatrix} 1 & 0 & 0 \\ 0 & C\phi_k & S\phi_k \\ 0 & -S\phi_i & C\phi_k \end{pmatrix}\begin{pmatrix} C\psi_k & S\psi_k & 0 \\ -S\psi_k & C\psi_k & 0 \\ 0 & 0 & 1 \end{pmatrix}$$

ψ_k, ϕ_k, θ_k represent the bodies known yaw, roll, and pitch Euler rotation angles with respect to the inertial reference frame. The transformation matrices $X[K_i(0)]$, $V[K_0(0)]$, $Y(1)$, $W[A_i(0)]$, $V[A_0(0)]$, and $Y(2)$ are defined in Table 1. $K_i(0)$, $K_0(0)$, $A_i(0)$, and $A_0(0)$ represent the position of the inner and outer gimbal angles of star tracker 2 and 3, respectively, at a known vehicle attitude defined by the direction cos matrix $A_{as}(k)$. From Eqs. (8) and (9), $\bar{T}_{22}$ and $\bar{T}_{33}$ are the second and third rows of the B_s matrix. The first row is $\bar{T}_1 = \bar{T}_2 \times \bar{T}_3$.

Since all the elements of the B_s and B_a matrices are known, the vehicle attitude is determined in terms of star tracker gimbal angles and the error matrix R can be computed from Eqs. (5) and (2).

Control Law Synthesis

According to Euler's theorem on rotation, the eigenvector of the R matrix $\bar{c}$, is the axis about which the vehicle is rotated to obtain the commanded position. The angle through which it is rotated about this axis is Φ. Reference 1 synthesizes a general control law which will force the vehicle to rotate about the eigenvector. This paper is concerned with a form of this general control law such that the control voltage to the torquers $Z_a(1)$, $Z_a(2)$, and $Z_a(3)$ and the wheel velocities must not exceed preassigned values but the system response must be fast. The control law mechanized is of the form

$$Z_a(I) = -\frac{J_a(I)Z(\max)}{J_a(\max)}\left[\mathrm{Sat}(\Phi;\Phi_s)c(I) + \frac{\omega_a(I)}{\omega_a(\max)}\right] \quad I = 1,2,3 \quad (10)$$

$Z_a(\max)$, $J_a(\max)$, $\omega_a(\max)$ are the max values of control torque, body inertia, and body rate respectively. The term $\mathrm{Sat}(\Phi,\Phi_s)$ is a gain term derived from the error matrix R:

$$\begin{aligned} \mathrm{Sat}(\Phi,\Phi_s) &= 1 \text{ for } \Phi \geq \Phi_s \\ &= \Phi/\Phi_s \text{ for } \Phi < \Phi_s \end{aligned} \quad (11)$$

The system saturation level is thus set by this term. Since $Z_a(\max)$, $J_a(\max)$, $\omega_a(\max)$ are constants the control law can be simplified to

$$Z_a(I) = -K_1(I)[\mathrm{Sat}(\Phi,\Phi_s)c(I) + K_2\omega_a(I)]I = 1,2,3 \quad (12)$$

The terms of $c(1)$, $c(2)$, and $c(3)$ are the components of the eigenvector $\bar{c}$ in the respective body axes and are given by

$$c(1) = \frac{1}{2}\left(\frac{R_{23} - R_{32}}{\sin\Phi}\right) \qquad c(2) = \frac{1}{2}\left(\frac{R_{31} - R_{13}}{\sin\Phi}\right)$$
$$c(3) = \frac{1}{2}\left(\frac{R_{12} - R_{21}}{\sin\Phi}\right) \quad (13)$$

where R_{12}, R_{21}, R_{23}, R_{32}, R_{31}, and R_{13} refer to the off-diagonal terms of the R matrix. If the vehicle is slewing about the eigenvector, then these components $c(I)$ will remain constant. Stored initial momentum, disturbance torques, or a nonsymmetrical mass configuration will cause the eigenvector components to vary with time.

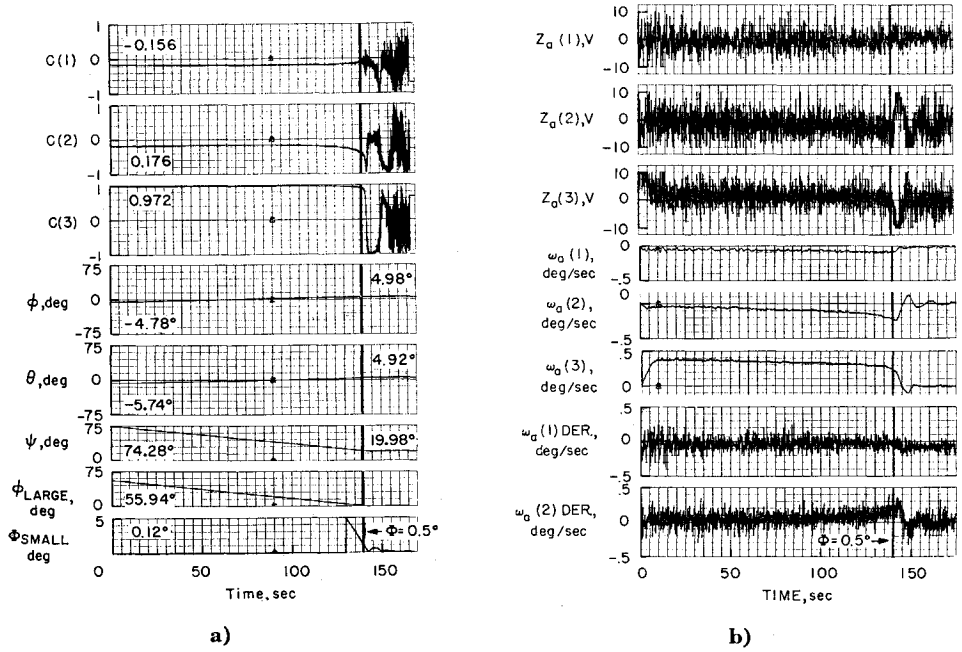

a) b)

Fig. 4 Gyro rate damping.

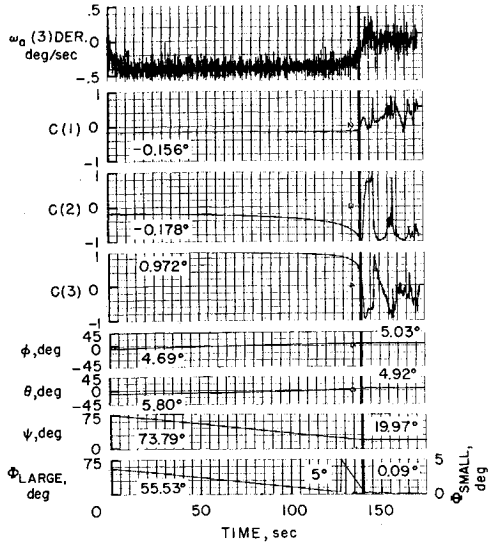

a)

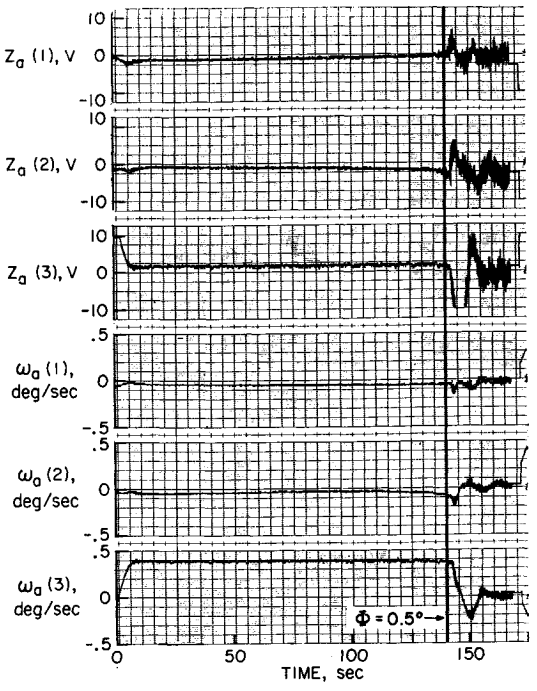

b)

Fig. 5 Derived rate damping.

The angle to go Φ is derived from the R matrix and is given by

$$\Phi = \cos^{-1} \tfrac{1}{2}(R_{11} + R_{22} + R_{33} - 1) \tag{14}$$

where R_{11}, R_{22}, and R_{33} are the diagonal terms of the error matrix R. If the vehicle is rotating about the eigenvector this angle should be a decreasing function of constant slope. The final value of Φ gives the system pointing error.

When the vehicle is within the saturation region ($\Phi > \Phi_s$), the control law is given by Eq. (14). When the vehicle is outside the saturated region [$\mathrm{Sat}(\Phi,\Phi_s) = \Phi|\Phi_s$], the Φ term in the numerator of this expression cancels the $\sin\Phi$ term in the denominator of $c(I)$ and the control law then becomes

$$Z_a(I) = -K_1(\mathrm{I})[q(I)/\Phi_s + K_2\omega_a(I)]I = 1,2,3 \tag{15}$$

where $q(I)$ is given by

$$q(1) = \tfrac{1}{2}(R_{23} - R_{32}) \qquad q(2) = \tfrac{1}{2}(R_{31} - R_{13})$$
$$q(3) = \tfrac{1}{2}(R_{12} - R_{21}) \tag{16}$$

A block diagram showing the elements of the control system and the procedure by which the control torque is generated is shown in Fig. 3. The position information from the star tracker gimbal angle transducers and the rate information from the rate gyros are sent in analog form to an analog to digital linkage associated with the digital computer. The proper matrix operations are performed on the digital position information and the A_{as} matrix is generated. This is multiplied with the commanded A_{ds} matrix and the error matrix R is generated. From the error matrix the components of the eigenvector to go is 5° and less. Also shown on the figures is the point at which the table reaches Φ, which is set at 0.5°. These test results were outputed from the digital computer, through the digital to analog linkage, to a strip chart recorder. The data were determined once every computation cycle (35 ms). A printout was made at the beginning and end of each slew. The numerical values obtained are also shown in Figs. 4–6.

Rate Gyro Damping Curves

Figure 4 shows the control system operating with damping obtained from rate gyroscopes. The table is initially positioned at Euler angles of −4.78° in roll, −5.74° in pitch, and 74.28° in yaw and is commanded to slew to 5.0° in roll and pitch and 20° in yaw. This command gives an angle to go of 55.94°. The time history of Φ_{LARGE} indicates that it decreases with a constant negative slope toward zero as predicted by the theory. Φ_{SMALL} shows that the system has two overshoots and settles to within 0.12° of the commanded value. The final values of the Euler angles are also an indication of the system pointing accuracy. It is observed from the Euler angle trace that the system error in the roll and yaw axis was 0.02°and in the pitch axis 0.08°.

For this run, the initial orientation of the eigenvector, with respect to the table roll, pitch, and yaw axes is 18°, 79°55,′ and 13°25′, respectively. This orientation is as expected since the major component of the command is about the yaw axis. The time history of the components of the eigenvector in the body coordinate frame show they remain nearly constant during the slew until $\Phi = \Phi_s$. When $\Phi = \Phi_s$ the control law is switched to drive the R matrix to the identity $\bar{c}$ and the error angle Φ are obtained and these are combined with the body rate information to generate the desired control law. The control signals are sent through the digital to analog linkage and to power amplifiers which drive the reaction wheel torquers.

The basic control law was investigated with body rate information obtained in two different ways. Body rate information obtained from rate gyroscopes was considered the basic mode of operation. This type of control was then compared to a system in which the body rate signal was derived from the A_{as} matrix.

Body Rate Derivation from the A_{as} Matrix

The body rate is derived from the A_{as} matrix by the use of the following relationship

$$\dot{A}_{as} = S(\omega_a)A_{as} \tag{17}$$

$S(\omega_a)$ is a skew-symmetric matrix and is given by:

$$S(\omega_a) = \begin{pmatrix} 0 & \omega_a(3) & -\omega_a(2) \\ -\omega_a(3) & 0 & \omega_a(1) \\ \omega_a(2) & -\omega_a(1) & 0 \end{pmatrix} \tag{18}$$

$\dot{A}_{as}$, the time derivative of A_{as}, is approximated by

$$\dot{A}_{as} = [A_s(n) - A_{as}(n+1)]/T \tag{19}$$

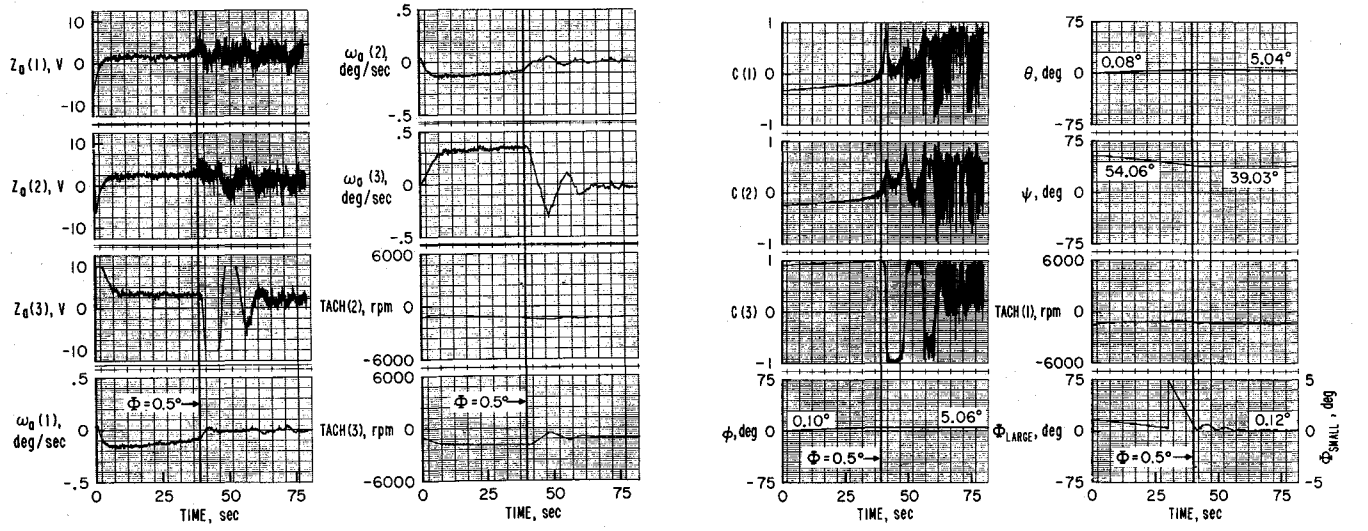

Fig. 6 System operating with initial momentum.

where $A_{as}(n)$ and $A_{as}(n+1)$ are the values of the A_{as} matrix at the beginning and end of a time interval specified by T. The matrix equation then takes the form

$$\begin{bmatrix} 0 & \omega_a(3) & -\omega_a(2) \\ -\omega_a(3) & 0 & \omega_a(1) \\ \omega_a(2) & -\omega_a(1) & 0 \end{bmatrix} = \left[\frac{A_{as}(n) - A_{as}(n+1)}{T}\right][A_{as}(n)]^t = \left[\frac{I - A_{as}(n+1)A_{as}(n)^t}{T}\right] \quad (20)$$

The three body rates $\omega_a(1)$, $\omega_a(2)$, $\omega_a(3)$ are obtained from this relationship.

The two types of control using different methods to obtain body rate were mechanized and the results compared. The system deriving rate from the direction cosine matrix is considered as a backup system should the rate gyroscopes fail. The control system using gyro damping was also evaluated with initial stored momentum.

Test Procedures and Results

The test results of this mechanization are shown in Figs. 4–6. The basic criteria under which the control system is evaluated is that the components of the eigenvector in the body axes $c(1)$, $c(2)$, and $c(3)$ remain constant from the beginning of a slew until $\Phi = \Phi_s$ and that the angle to go Φ_{LARGE} approach zero in a linear manner. These parameters are shown in Figs. 4, 5, and 6 together with the table Euler angles ϕ, θ, and ψ as derived from the direction cos matrix, A_{as}, the control voltages to the motors $Z_a(1)$, $Z_a(2)$, and $Z_a(3)$ and the body angular rates $\omega_a(1)$, $\omega_a(2)$, $\omega_a(3)$. Since system nulling characteristics as well as wide angle slew characteristics were of interest the angle to go Φ is shown in two scales. Φ_{LARGE} shows the angle to go during the complete slew and has a max level of 75°. Φ_{SMALL} shows the system operation when the angle irrespective of the eigenvector control is as shown by Eq. (17). The values of $c(1)$, $c(2)$, and $c(3)$ become very noisy at this point. Since $\bar{c}$ is defined as a unit vector fixed in space, the square root of the sum of the squares of its components should equal one. This is very close to being the case in this run, the discrepancy arising from noise on the input signals.

The control voltage for the axis about which the error is a max initially saturates and then decreases to a level necessary to maintain the ω_a(max) rate. This occurs about the yaw axis in Fig. 4. The average control voltage about the roll and pitch axis is proportionately lower as determined by the values of the $\bar{c}$ components.

Derived Rate Damping Curves

As has been previously shown by Eq. (22), it is possible to obtain body rates from the A_{as} matrix. This rate information could be used as a backup system to the gyros. Figure 5 shows the system operating with derived rate damping. The slew command shown in this figure is the same as shown in Fig. 4. Of interest in this run is the shape of the derived rate curves $\omega_a(I)$ DER, as compared to the body rates obtained from the gyroscopes. It is observed that the derived rate information is noisy when compared to the gyro rate information. This is because it is obtained by essentially a time differentiation process. In order to reduce the noise the A_a matrix was averaged over a 100 ms time period. The averaging process filters the rate information but does not introduce enough lag to affect system stability. Without this filtering, the rate information is completely masked by the noise. The noise present on the rate signal makes the control voltage to the reaction wheels noisy as is shown by their time histories. However, since the frequency response of the system is below one Hertz, the noise has a minor affect on system performance as is shown by the trace of the $\bar{c}$ components and by Φ_{LARGE}

The linearity of $c(1)$, $c(2)$, and $c(3)$, while not as good as in the previous run with gyro damping, is still acceptable. The angle between the orientation of the $\bar{c}$ axis at time $t = 0$ and its orientation at time $t = 120$ sec is 20°. If the system were controlling perfectly and there were no disturbance torques the angle would be zero.

From the traces for Φ_{SMALL} in Fig. 5 it is observed that the system nulling and holding characteristic is about as good as in Fig. 4.

Initial Momentum Curves

Figure 6 shows the affect of initial stored momentum on the control system. The time histories of the inertia wheel tachometer traces, tach(1), tach(2), and tach(3) show that the initial rates of the roll, pitch, and yaw reaction wheels were 1600 rpm, 1150 rpm, and 1050 rpm, respectively. The final wheel velocities were very close to these initial values. The difference is due to disturbance torques acting on the table. From the time history of Φ_{SMALL} it is observed that it is well behaved with a final pointing error of 0.12°. The motor control voltages $Z_a(1)$, $Z_a(2)$, and $Z_a(3)$ show the offset levels

necessary to maintain the wheels spinning at the initial rate. The traces of the eigenvector components in Fig. 6 show that the initial stored momentum causes the eigenvector orientation to vary during the slew as predicted by the theory. However, this variation is not excessive and does not introduce any instabilities into the control system. The curves in Fig. 6 show that the system performance does not greatly deteriorate when operating with initial angular momentum.

Concluding Remarks

The test results shown in Figs. 4–6 show that the wide angle attitude control system based on Euler's theorem on rotation performs as predicted by the theoretical analysis. The test results indicate that the system can stabilize the body with a high degree of accuracy at the target position. It was also shown that a redundant type of control system package could be implemented which would avoid a flight abort in case of gyroscope failure.

The type of control system shown in this mechanization could be used very effectively on a vehicle such as the OAO where it is desired to command the spacecraft through large angles. The system has proven global stability and the path it will take during a slew is well-behaved and predictable. It also results in a direct motion about a single axis rather than about three axes separately which may make it a desirable type of control for a manned vehicle.

References

[1] Meyer, G., "On the Use of Euler's Theorem on Rotations for the Synthesis of Attitude Control Systems," TN D-3643, 1966, NASA.

[2] Goldstein, H., *Classical Mechanics*, Addison-Wesley, Reading, Mass., 1959.

JULY 1970 J. SPACECRAFT VOL. 7, NO. 7

Strapdown Inertial Attitude-Indication Evaluations

JEROLD P. GILMORE* AND RICHARD A. MCKERN†
Charles Stark Draper Laboratory, Massachusetts Institute of Technology, Cambridge, Mass.

Results of a test-evaluation study of the strapdown mechanization for inertial-grade attitude indication are presented. An experimental gyro test package, dynamic test facility and computational attitude algorithm are described. Static and dynamic test results obtained using real-time monitoring are presented with error propagation profiles. Single-degree-of-freedom gyros were mechanized in a digital torque-to-balance control loop. The gyro incremental output data were processed in real-time in a digital computer to correct for instrument error sources and perform the attitude transformation update. Whole-number quaternion algorithms were developed and performance trade offs for various algorithm parameters are presented with confirming test results. The bounds of realizable system performance are shown to be dependent on instrument parameter stability and algorithm bandwidth. Performance in various application environments may be projected by the results presented.

Introduction

UNLIKE other studies[1,2] this program employed integrated real-time system test evaluations to explore the inertial-attitude indication capabilities of the pulse-torque-to-balance gyro strapdown configuration. Thus, a structure-mounted gyrotest package, a dynamic test table, torquing electronics and associated power supplies, and a computational facility were assembled. Similarly, studies on instrument error sources and attitude reference algorithms were conducted and synthesized into operating software. Static and dynamic tests were then devised and conducted with an aim towards determining hardware-software tradeoff performance criteria and limitations.

System Test Configuration

Test Package

The experimental test package shown in Fig. 1 contains three orthogonally mounted 18-size Inertial Reference Integrating Gyroscopes (18IRIG). Each gyro is mounted in an alignment fixture and normalized with a signal-generator preamplifier, suspension and quadrature networks and a temperature controller. An optical cube mounted on the frame is the alignment reference, allowing determination of the test package orientation relative to azimuth and local-vertical. The frame is aluminum with coolant passages for air-to-liquid heat exchanger operation and is shrouded for environment isolation. Three sets of pads form a triad of planes that mate with the gyro alignment fixture. This fixture allows independent adjustment of the gyro input axis (IA) about its spin axis (SA) and its output axis (OA). The package form factor allows for substitution within the gimbals of an Apollo Inertial Measurement Unit for special dynamic testing. In this evaluation the package was mounted on the precision 4 axis test table via a high-thermal resistance, adjustable alignment plate. Test-table positioning accuracy is calibrated to 2 arc sec. Constant rates of up to 1 rad/sec and oscillatory frequencies of up to 10 Hz can be obtained about two of its rotary axes. Thus, precision static orientation, rate, and oscillatory input capabilities allowed gyro drift parameter, scale-factor, and end-to-end dynamic performance test determinations. The test configuration, the computer, and the dynamic test table on which the experimental test package is mounted are shown in Fig. 2.

Presented as Paper 69–849 at the AIAA Guidance Control, and Flight Mechanics Conference, Princeton, N. J., August 18–20, 1969; submitted August 27, 1969; revision received February 11, 1970. Conducted at the Massachusetts Institute of Technology, Charles Stark Draper Laboratory under the auspices of the NASA Manned Space Flight Center, Contract NAS 9-6823.

* Director, Apollo Inertial Subsystems.
† Assistant Director, Systems Analysis.